

Finite element model updating of long-span cable-stayed bridge by Kriging surrogate model

Jing Zhang^{1,2a}, Francis T.K. Au^{2b} and Dong Yang^{*1,2}

¹Department of Civil Engineering, Hefei University of Technology, Hefei, Anhui Province, China

²Department of Civil Engineering, The University of Hong Kong, Pokfulam Road, Hong Kong, China

(Received May 2, 2019, Revised August 26, 2019, Accepted November 17, 2019)

Abstract. In the finite element modelling of long-span cable-stayed bridges, there are a lot of uncertainties brought about by the complex structural configuration, material behaviour, boundary conditions, structural connections, etc. In order to reduce the discrepancies between the theoretical finite element model and the actual static and dynamic behaviour, updating is indispensable after establishment of the finite element model to provide a reliable baseline version for further analysis. Traditional sensitivity-based updating methods cannot support updating based on static and dynamic measurement data at the same time. The finite element model is required in every optimization iteration which limits the efficiency greatly. A convenient but accurate Kriging surrogate model for updating of the finite element model of cable-stayed bridge is proposed. First, a simple cable-stayed bridge is used to verify the method and the updating results of Kriging model are compared with those using the response surface model. Results show that Kriging model has higher accuracy than the response surface model. Then the method is utilized to update the model of a long-span cable-stayed bridge in Hong Kong. The natural frequencies are extracted using various methods from the ambient data collected by the Wind and Structural Health Monitoring System installed on the bridge. The maximum deflection records at two specific locations in the load test form the updating objective function. Finally, the fatigue lives of the structure at two cross sections are calculated with the finite element models before and after updating considering the mean stress effect. Results are compared with those calculated from the strain gauge data for verification.

Keywords: cable-stayed bridge; fatigue life; health monitoring; mean stress effect; model updating; surrogate model

1. Introduction

Long-span cable-stayed bridges have become popular for major crossings (Xie *et al.* 1997). Because of their complexity, the finite element (FE) method is often considered the only feasible way for structural modelling and analysis (Lertsima *et al.* 2004, Li *et al.* 2017). However, in the development of FE models, various simplifying assumptions are normally made, and hence discrepancies may arise from various sources, including: (a) simplification of structural geometry; (b) material properties such as elastic modulus, sectional area, etc.; (c) inaccurate joint and boundary conditions; and (d) non-conformity of model order and discretization errors (Mottershead and Friswell 1993, Matta and De Stefano 2012). While conservative simplifying assumptions are acceptable for design purposes, more sophisticated numerical models are often required to reflect the actual structural behaviour. The uncertain physical parameters of an FE model should be

updated so as to improve the accuracy of predicted responses (Arora 2014).

There are two categories of FE model updating methods, namely indirect method and iterative method. In the direct method, the elements of stiffness and mass matrices are directly updated in a single-step procedure. No iteration is needed but the updated mass and stiffness matrices have little physical meaning and cannot be related to physical changes in the original model (Friswell and Mottershead 1995). In the iterative method, FE model updating is formulated as an optimization problem with objective functions so that iteration is terminated once the stipulated conditions are satisfied. The discrepancies between the numerical predictions and field measurements of modal parameters are most commonly adopted to form the objective functions (Wei 1990, Vahidi *et al.* 2019), including natural frequency, mode shape, damping ratio as well as their derived parameters such as mode shape curvature and modal flexibility. However, the algorithm may fail to converge if there are too many objective functions specified in the algorithm or if the tolerances are made too stringent. Moreover, the structural FE models are often built using commercial FE packages. In other words, each cycle of iteration involves executing the FE package with the parameters updated, which can be computationally intensive. Therefore, it is desirable to devise a more efficient method for developing baseline models.

*Corresponding author, Associate Professor

E-mail: yangdong@hfut.edu.cn

^a Associate Professor

E-mail: zhangj@hfut.edu.cn

^b Professor

E-mail: francis.au@hku.hk

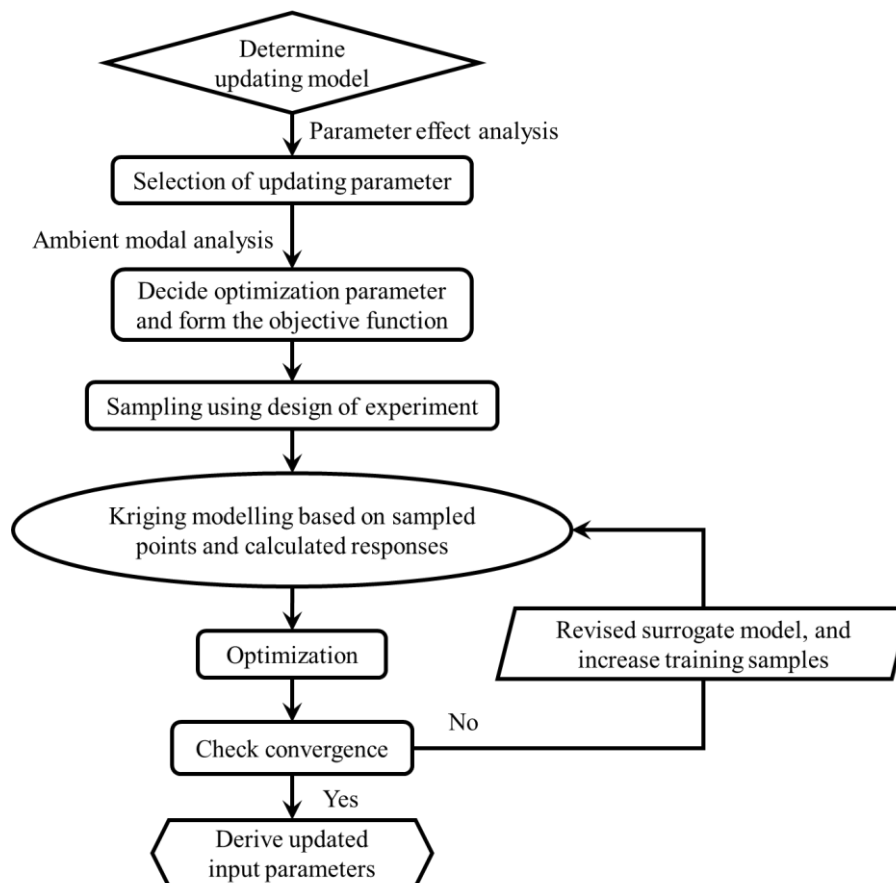


Fig. 1 Updating procedure using the Kriging surrogate model

One way to overcome the extensive FE computations during the development of baseline model is to replace the FE model by an approximate but efficient surrogate or meta-model (Kalita *et al.* 2018). The surrogate model has been promoted as a promising method for FE model updating (Shao and Krishnamurty 2008, Hwang *et al.* 2018) and damage identification (Gao *et al.* 2012). In essence, the surrogate model examines various design variables and their responses in order to identify the design variables that give the most accurate response. Using this, the original sophisticated FE model can be replaced by a simplified surrogate model constructed by statistical approximation (Myers 1999). In the search for a promising method for FE model updating, an optimization approach with the response surface method using an explicit polynomial instead of a complicated implicit performance function has been promoted (Ren and Chen 2010, Ren *et al.* 2010), but the order of polynomial to construct the surface has to be determined by trials and the accuracy is doubtful in highly nonlinear problems (Basaga *et al.* 2012). As a spatial local interpolation method, Kriging model is actually a linear regression analysis method, based on regionalized variable unbiased and optimal estimates, the weighted coefficient of each sample point is calculated and linearly combined, then the best estimator can be achieved (Qin *et al.* 2019, Simpson *et al.* 2001). Kriging model has both local and global statistical characteristics, which makes Kriging method more universal and more suitable for sorting and

analyzing known trends and dynamics (Dubourg *et al.* 2011, Sakata *et al.* 2008).

Kriging model has been extensively applied to various branches of engineering (Khodaparast *et al.* 2011, Zhang *et al.* 2012) with the development of Kriging toolbox based on Matlab-DACE (Lophaven *et al.* 2002). Compared to the conventional response surface models, the constant “global” Kriging model is demonstrated to be more accurate (Simpson *et al.* 1998, Gaspar *et al.* 2014). It is particularly useful when applied to the problems with highly dimensional input and response. In this study, the Kriging model which can approximate multivariate input/output relationships of time-consuming physics-based FE models is proposed for physical parameters updating. The proposed method is simple and fast so that it can be easily implemented in practice. The updating parameters are selected on the basis of the prior knowledge about the structural behaviour first, and then the sensitivity of different parameters can be evaluated from the sampled data by performing a parameter effect analysis based on analysis of variance. With the static response features and the dynamic properties of natural frequencies to form the updating objective functions, the optimization problem can be solved with the Kriging model established using sequential quadratic programming without any further FE simulations. The proposed method will be verified by numerical examples and its use in fatigue life assessment considering the mean stress effect (Zhang and Au 2013) will be examined in particular.

2. Kriging model-based finite element model updating

The Kriging model is a half-parametric prediction model as no particular mathematical model is needed for its application. The fitted surface formed also passes through all the sampling points used to estimate the unknown points. For each training sample, the predicted value provided by the function of the model is very accurate. For the others, not only is the predicted value provided but also the variances are given, which can allow the user to weigh its accuracy. With minimal variance of the prediction model, local estimation can be achieved with satisfactory fitting results for nonlinear problems.

The main steps of model updating based on Kriging model are shown in Fig. 1 and elaborated below:

- (a) Determine the input parameters to be updated, which are the physical parameters of FE model.
- (b) Define the number of ‘levels’ for each input parameter by using the techniques of design of experiments.
- (c) In the design space, obtain the output features from FE analyses, including the static and dynamic responses.
- (d) Create the Kriging model for the structure using the input parameters and output features obtained in Step (c).
- (e) Construct the objective functions to be minimized in the equivalent optimization problem.
- (f) Update the physical parameters by minimizing the objective functions using the Kriging model established.

2.1 Theory of Kriging model

The essence of Kriging model applied is briefly described here. Kriging model is a surrogate model interpolated from a group of observation dataset of input and output. This model is able to approximate the “black box” model of input parameters and output features. It consists of two main parts, including the modelling of linear regression and stochastic process. The relationship between the output $\mathbf{Y}(\mathbf{x})$ and the design variable \mathbf{x} can be described as (Sacks *et al.* 1989):

$$\mathbf{Y}(\mathbf{x}) = \mathbf{F}(\mathbf{x})\boldsymbol{\beta} + \mathbf{Z}(\mathbf{x}) \quad (1)$$

where the product of design matrix $\mathbf{F}(\mathbf{x})$ as a function of design variable \mathbf{x} and the regression coefficient vector $\boldsymbol{\beta} = [\boldsymbol{\beta}_1, \dots, \boldsymbol{\beta}_m]$ denotes the regression model that approximates the global trend of the design space, and $\mathbf{Z}(\mathbf{x})$ is the system deviation considered as a stochastic process that should be independent and identically distributed, e.g. Gaussian stationary process. The statistical characteristics of $Z_l(\mathbf{x})$ denoting the system deviation for the l -th column of response include:

$$E[Z_l(\mathbf{x})] = 0 \quad (2)$$

$$\text{Var}[Z_l(\mathbf{x})] = \sigma_l^2 \quad (3)$$

where σ_l^2 is the process variance. The covariance of the process can be defined as:

$$\text{Cov}[Z_l(\mathbf{x}^i), Z_l(\mathbf{x}^j)] = \sigma_l^2 [R(\mathbf{x}^i, \mathbf{x}^j)] \quad (4)$$

in which n is the number of coordinate components (design variables), and $R(\mathbf{x}^i, \mathbf{x}^j)$ is the spatial correlation function with many choices provided for model approximation. Among them, the Gaussian correlation function is the most popular, and is hence adopted here:

$$R(\mathbf{x}^i, \mathbf{x}^j) = \exp\left(-\sum_{k=1}^n (\theta_k |x_k^i - x_k^j|^2)\right) \quad (5)$$

where x_k^i denotes the k -th component of x_i , and θ_k is a correlation parameter to ensure high model flexibility. For an arbitrary set of $\mathbf{x}^* = [\mathbf{x}_1 \dots \mathbf{x}_d]^T$ and the output vector $\hat{\mathbf{y}} = [\mathbf{y}_1 \dots \mathbf{y}_d]^T$, the optimized coefficient matrix of regression estimation of parameters $\boldsymbol{\beta}^*$ can be written as:

$$\boldsymbol{\beta}^* = (\mathbf{F}^T \mathbf{R}^{-1} \mathbf{F})^{-1} (\mathbf{F}^T \mathbf{R}^{-1} \mathbf{Y}) \quad (6)$$

where \mathbf{R} is the correlation matrix of the training points given as:

$$\mathbf{R} = \begin{bmatrix} R(x_{l1}, x_{l1}) & R(x_{l1}, x_{l2}) & \cdots & R(x_{l1}, x_{ld}) \\ R(x_{l2}, x_{l1}) & R(x_{l2}, x_{l2}) & \cdots & R(x_{l2}, x_{ld}) \\ \vdots & \vdots & \cdots & \vdots \\ R(x_{ld}, x_{l1}) & R(x_{ld}, x_{l2}) & \cdots & R(x_{ld}, x_{ld}) \end{bmatrix} \quad (7)$$

Here, the correlation parameter θ_k is the only unknown parameter that has to be obtained by maximizing of a function ψ as a function of θ_k and R :

$$\psi = \frac{n \ln(\overline{\sigma^2}) + \ln |\mathbf{R}|}{2} \quad (8)$$

Then the predicted l -th component \hat{y}_l of the response vector $\hat{\mathbf{y}}$ can be determined as:

$$\hat{y}_l = \mathbf{F}(\mathbf{x}^*) \boldsymbol{\beta}_l^* + (\mathbf{r}(\mathbf{x}^*))^T \mathbf{R}^{-1} (\mathbf{y}_l - \mathbf{F} \boldsymbol{\beta}_l^*) \quad (9)$$

where $\mathbf{r}(\mathbf{x}^*)$ is a vector denoting the correlation between the \mathbf{x}^* and all the known training points, i.e.

$$\mathbf{r}(\mathbf{x}^*) = [R(\mathbf{x}_1, \mathbf{x}^*), R(\mathbf{x}_2, \mathbf{x}^*), \dots, R(\mathbf{x}_d, \mathbf{x}^*)]^T \quad (10)$$

So far, all the response features can be estimated accurately.

2.2 Sampling

The basic process to create a Kriging model for the FE model consists in the calculation of feature values at various sampling points in the parameter space by performing an “experiment” at each of these points. Therefore a proper design of experiment, which selects the key factors that vary in certain ranges to evaluate the influence on the output values, is often carried out to obtain the most information with the least cost. There are various kinds of experimental design such as the factorial design, orthogonal design, uniform design, and so on. Among them, the

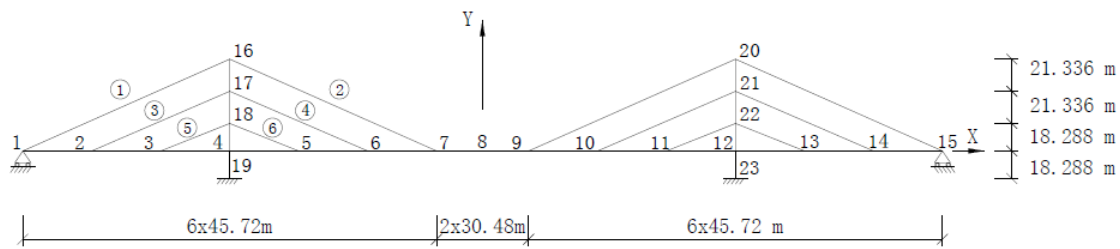


Fig. 2 Example 1: A simple hypothetical cable-stayed bridge

method of uniform design (Fang and Wang 1993, Montgomery 2017) is considered as an efficient fractional factorial design to uniformly arrange a reasonable number of design points in the domain in order to achieve the necessary accuracy. A uniform design is one in which the design points are scattered uniformly in the experimental domain. Such a design has the advantages that (Li *et al.* 2004): (a) within a small number of experimental runs, a significant amount of information can be obtained to explore the relationship between the response and the contributing factors; and (b) it is robust to the underlying model assumption, which means that it performs well even if the form of the regression model is unknown.

2.3 Selection of parameters

To update an FE model, the physical parameters of material and/or geometrical properties such as Young's moduli, moments of inertia, mass densities, etc. need to be adjusted in the light of field measurements. The success of FE model updating depends heavily on the proper selection of physical parameters to calculate the structural response features. However, it is not easy to determine the number of parameters to be selected for updating. To avoid any ill-conditioned numerical problems, sufficient parameters are selected on the basis of prior knowledge about the structural behaviour. There are two basic approaches for the initial selection of physical parameters, namely the empirical approach and the sensitivity-based approach. The empirical approach is fundamentally correct as it is based on the knowledge of approximations built into the initial FE model (Jaishi and Ren 2007). In most practical applications, the initial FE models are constructed based on available drawings of the structure itself. The parameters can be selected based on empirical knowledge of the initial model so that the less accurate parameters are selected for updating. However, this empirical process depends very much on engineering judgment. As it is impractical to inspect every detail of a real structure, the selection of parameters requires considerable insight, and a trial and error approach is often used (Jaishi *et al.* 2007).

In the sensitivity method, the parameters are so chosen that the response is sensitive to the parameters and hence the selected parameters should be able to clarify the ambiguity of the model. In the FE model updating based on Kriging model, the sensitivity of different parameters can

be evaluated from the sampled data by performing an analysis of variance. The theoretical foundation of analysis of variance is that the total variance of the output features can be decomposed into a sum of partial variances, each of which representing the effect of varying an individual factor independently from the others. To evaluate the significance of each parameter and to identify the most influential input parameters, F -test (Ahmadian *et al.* 1997) is adopted in analyzing variance for comparison of factors of system deviation, of which the significance F_A is distributed approximately as $F(f_A, f_e)$ given by

$$F_A = \frac{S_A/f_A}{S_e/f_e} \sim F(f_A, f_e) \quad (11)$$

where S_A and S_e are the sum of squares of system deviation and deviation of experiment of factor A , respectively. f_A and f_e are their corresponding degrees of freedom. Thus when there are few factors, full factorial design can be employed to evaluate the significance. However, when it becomes computationally intensive to process the full factorial design, orthogonal design can be implemented because the parameters are uncorrelated with minimum variance and hence maximum accuracy.

2.4 Optimization strategy

Optimization problems can be categorized into constrained and unconstrained forms, depending on whether constraints are imposed on the optimization function or not. In a constrained optimization problem, the objective function $f(x)$ to be minimized may be subject to constraints in the form of equality constraints $G_i(x) = 0$ ($i = 1, 2, \dots, m_e$), inequality constraints $G_i(x) \leq 0$ ($i = m_e+1, m_e+2, \dots, m$) as well as lower and upper parameter bounds x_{lb} and x_{ub} respectively. A constrained optimization problem is often transformed to simpler sub-problems that can be solved and used in further iteration. A constrained problem may also be formulated as an unconstrained problem by using a penalty function to impose the necessary conditions near or beyond the constraint boundary. Therefore a sequence of parameterized unconstrained optimization problems can be used to solve the constrained problem, which converges to the constrained problem in the limit. However, these methods are considered to be relatively inefficient. They are usually replaced by methods that focus on the solution of the Kuhn-Tucker equations, which are necessary conditions

Table 1 Example 1: Structural parameters of the hypothetical cable-stayed bridge

Parameter	Girder	Tower	Cable
Modulus of elasticity (MPa)	198201.6	198201.6	198201.6
Moment of inertia (m ⁴)	1.1307	0.2106 (top); 0.3452; 0.4315; 0.5179 (bottom)	-
Sectional area (m ²)	0.3193	0.2025 (top); 0.2276; 0.2694; 0.2973 (bottom)	0.0420 (exterior); 0.0162 (interior) 3.2251 (exterior); 1.2404 (interior)
Dead load (kN/m)	87.5591	-	-

Table 2 Example 1: Modal frequencies and displacements in static load test of the initial FE model

Modal frequencies (Hz)									
f_1	f_2	f_3	f_4	f_5	f_6	f_7	f_8	f_9	f_{10}
3.965	10.90	12.69	13.69	15.59	16.22	18.76	21.29	21.85	24.51
7	9	0	9	0	2	6	1	1	8
Maximum static displacements (m)									
Node 7					Node 8				
-0.42503					-0.46166				

for optimality for a constrained optimization problem. These methods are commonly referred to as the sequential quadratic programming methods (Sahin and Bayraktar 2014), which have been applied in this study by the optimization toolbox in MATLAB 8.0 (2012).

3. Example 1: A simple cable-stayed bridge

The efficiency and accuracy of the proposed method are firstly verified by a simple hypothetical cable-stayed bridge as shown in Fig. 2 (Cheng 2010). The structural parameters of the three-span cable-stayed bridge are listed in Table 1. The height of each tower is 79.248 m and the sectional properties of four segments are different. The deck is monolithic with the tower at the intersection and symmetry is assumed for simplicity. Using the commercial package ANSYS Multiphysics 12.0 (2009), the FE model of the bridge is established. The stiffening girder is divided into 84 beam elements while the towers are divided into 8 beam elements. Each cable is treated as a single link element.

Table 2 shows that simulated dynamic and static properties of the bridge based on the initial FE model having the structural parameters shown in Table 1. The dynamic properties include the first 10 modal frequencies f_1 to f_{10} . Assume that static loading tests using an axle load of 1000 kN are conducted on the bridge to monitor the displacements at critical locations such as Nodes 7 and 8 so that the maximum displacements are extracted. In actual construction, tolerances are allowed in various parameters. For example, because of various requirements in the specifications, contractors normally provide concrete with higher strength than specified and hence higher modulus of

Table 3 Example 1: Assumed variations of parameters in the “real” bridge

Structural component	Model parameters			
	Modulus of elasticity (MPa)	Moment of inertia (m ⁴)	Sectional area (m ²)	Dead load (kN/m)
Girder	+15%	-10%	-5%	+10%
Tower	+15%	-10%	-5%	-
Cable	-	-	-	-

Table 4 Example 1: Modal frequencies and displacements in static load test of the “real” bridge

Modal frequencies (Hz)									
f_1	f_2	f_3	f_4	f_5	f_6	f_7	f_8	f_9	f_{10}
4.136	11.37	13.15	14.26	16.19	16.83	19.33	21.84	22.73	25.45
4	9	3	4	2	0	4	7	6	2
Maximum static displacements (m)									
Node 7					Node 8				
-0.53605					-0.57847				

Table 5 Example 1: Selected parameters for updating FE model

No.	Model parameters	Allowable bounds (%)
1	Elastic modulus of girder (concrete)	±20
2	Elastic modulus of tower (concrete)	±20
3	Moment of inertia of girder	±30
4	Moment of inertia of tower	±30
5	Sectional area of girder	±20
6	Sectional area of tower	±20
7	Dead load of girder	±15

elasticity. Table 3 shows the assumed variations of parameters in the “real” bridge, while the corresponding dynamic and static properties of the “real” bridge are simulated and shown in Table 4. Hence the corresponding residuals of these quantities between the initial FE model and any trial model can be used to form the objective function for updating the initial FE model.

The parameters shown in Table 3 are selected for updating and reasonable ranges of variation are assumed as given in Table 5. In this example, the uniform design table $U_{28}^*(28^8)$ shown in Table 6 and the associated application table in Table 7 are used (Fang and Wong 1993) because of the small deviation D of 0.1550. The uniform design tables available are designated as $Un(q^s)$ or $U_n^*(q^s)$, where U means uniform design, n is the number of trials, q denotes the number of levels for each factor, s denotes the number of columns, and the asterisk denotes the preferred table with better uniformity for implementation. Tables 8 and 9 show that the FE model updated by Kriging model agrees well with properties of the “real” bridge with discrepancies below 2%, which ensures the physical meaning of parameters. For comparison, a quadratic polynomial response surface model is also used to update the FE model with the corresponding results given in Tables 10 and 11. Obviously the Kriging model performs much better.

Table 6 Uniform design table of $U_{28}^*(28^8)$

Level \ Factor	1	2	3	4	5	6	7	8
1	1	7	16	18	20	23	24	25
2	2	14	3	7	11	17	19	21
3	3	21	19	25	2	11	14	17
4	4	28	6	14	22	5	9	13
5	5	6	22	3	13	28	4	9
6	6	13	9	21	4	22	28	5
7	7	20	25	10	24	16	23	1
8	8	27	12	28	15	10	18	26
9	9	5	28	17	6	4	13	22
10	10	12	15	6	26	27	8	18
11	11	19	2	24	17	21	3	14
12	12	26	18	13	8	15	27	10
13	13	4	5	2	28	9	22	6
14	14	11	21	20	19	3	17	2
15	15	18	8	9	10	26	12	27
16	16	25	24	27	1	20	7	23
17	17	3	11	16	21	14	2	19
18	18	10	27	5	12	8	26	15
19	19	17	14	23	3	2	21	11
20	20	24	1	12	23	25	16	7
21	21	2	17	1	14	19	11	3
22	22	9	4	19	5	13	6	28
23	23	16	20	8	25	7	1	24
24	24	23	7	26	16	1	25	20
25	25	1	23	15	7	24	20	16
26	26	8	10	4	27	18	15	12
27	27	15	26	22	18	12	10	8
28	28	22	13	11	9	6	5	4

Table 7 Application table for $U_{28}^*(28^8)$

s	Column number							D
2	1	4						0.0545
3	1	2	5					0.0935
4	1	2	5	7				0.1074
5	1	2	3	7	8			0.1381
6	1	2	3	5	6	7		0.1578
7	1	2	3	5	6	7	8	0.1550

Table 8 Example 1: Updated parameters of “real” bridge by Kriging model

Structural component	Updated parameters by Kriging model							
	Modulus of elasticity		Moment of inertia		Sectional area		Dead load	
	Updated (GPa)	Diff (%)	Updated (m^4)	Diff (%)	Updated (m^2)	Diff (%)	Updated (kN/m)	Diff (%)
Girder	2.123	+7.123	1.076	-4.879	0.300	-6.003	96.426	+10.127
Tower	2.219	+11.968	0.190	-9.582	0.236	+16.548	-	-
Cable	-	-	-	-	-	-	-	-

Table 9 Example 1: Accuracy of results of updated FE model of “real” bridge by Kriging model

Output	Objective values	After updating	Discrepancy (%)
Modal frequencies (Hz)			
f_1	4.1364	4.1231	-0.32
f_2	11.379	11.343	-0.32
f_3	13.153	13.147	-0.05
f_4	14.264	14.229	-0.25
f_5	16.192	16.105	-0.54
f_6	16.830	16.739	-0.54
f_7	19.334	19.184	-0.78
f_8	21.847	21.669	-0.81
f_9	22.736	22.701	-0.15
f_{10}	25.452	25.456	0.02
Maximum static displacements (m)			
Node 7	-0.53605	-0.54445	1.57
Node 8	-0.57847	-0.58719	1.51

Table 10 Example 1: Updated parameters of “real” bridge by response surface method

Structural component	Updated parameters by response surface method							
	Modulus of elasticity		Moment of inertia		Sectional area		Dead load	
	Updated (GPa)	Diff (%)	Updated (m^4)	Diff (%)	Updated (m^2)	Diff (%)	Updated (kN/m)	Diff (%)
Girder	2.150	+8.483	0.817	-27.786	0.369	+15.694	81.026	-7.462
Tower	2.264	+14.221	0.251	+19.177	0.208	+2.780	-	-
Cable	-	-	-	-	-	-	-	-

Table 11 Example 1: Accuracy of results of updated FE model of “real” bridge by response surface method

Output	Objective values	After updating	Discrepancy (%)
Modal frequencies (Hz)			
f_1	4.1364	3.4284	-17.12
f_2	11.379	9.4064	-17.34
f_3	13.153	11.922	-9.36
f_4	14.264	12.552	-12.00
f_5	16.192	13.815	-14.68
f_6	16.830	14.437	-14.22
f_7	19.334	18.854	-2.48
f_8	21.847	19.645	-10.08
f_9	22.736	21.861	-3.85
f_{10}	25.452	22.916	-9.96
Maximum static displacements (m)			
Node 7	-0.53605	-0.28624	-46.60
Node 8	-0.57847	-0.32377	-44.03

4. Example 2: Ting Kau Bridge in Hong Kong

Ting Kau Bridge is a cable-stayed bridge forming part of Route 3 of the highway network in Hong Kong with a

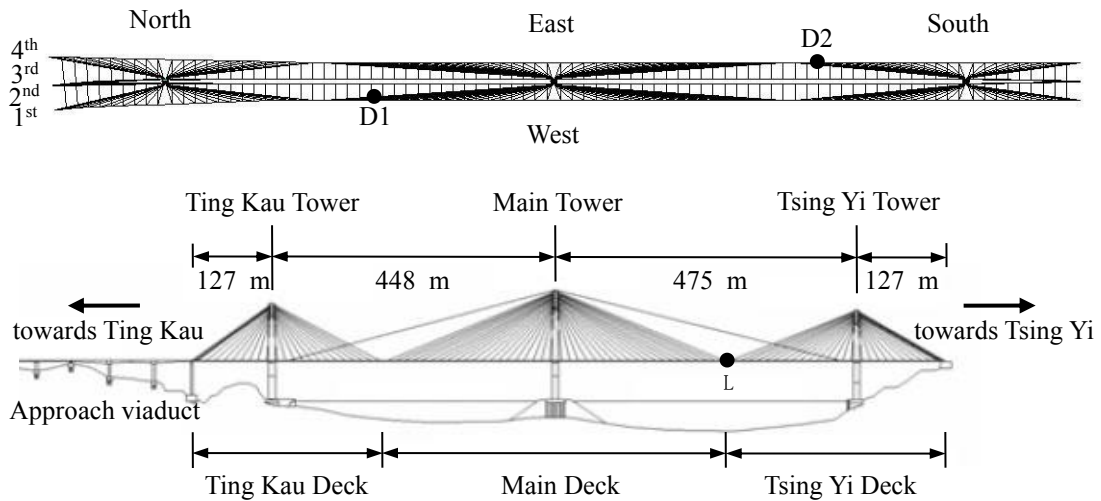


Fig. 3 Example 2: Schematic plan of Ting Kau Bridge in Hong Kong

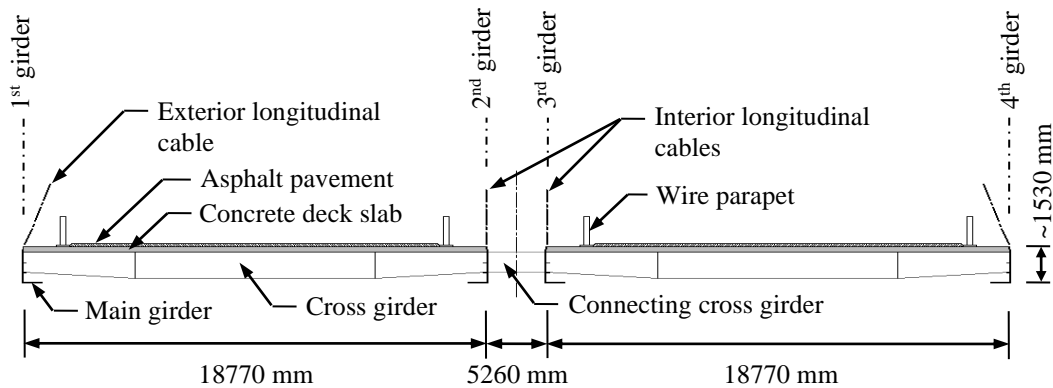


Fig. 4 Example 2: Typical arrangement of main deck (facing towards Ting Kau)

total length of 1,177 m. The Ting Kau main span and Tsing Yi main span are 448 m and 475 m respectively, while the two side spans are both 127 m. The bridge connects Ting Kau Island at the north and Tsing Yi Island at the south over Rambler Channel. The most prominent features of the bridge are perhaps the towers and cables. As shown in Fig. 3, there are three reinforced concrete towers, namely the Ting Kau Tower (162 m), Main Tower (168 m) and Tsing Yi Tower (162 m). Each tower consists of a mast that reduces its section in steps, and it is stabilized in the transverse vertical plane by stabilizing cables. The two decks are constructed by precast reinforced concrete panels that are joined by in-situ concrete, and supported by a grid of longitudinal main girders and transverse cross girders. For convenience in the subsequent discussions, the four longitudinal girders supported from four inclined cable planes emanated from three towers are labelled as '1st', '2nd', '3rd' and '4th'. A series of connecting cross girders installed at regular intervals are used to connect the two decks as shown in Fig. 4.

The FE model of Ting Kau Bridge is constructed using ANSYS Multiphysics 12.0. The deck, towers and struts are modelled by beam elements while the stay cables are

modelled by link elements taking into account the sag effect. The complete grid beam model consists of 5,594 BEAM4 and BEAM44 elements for the deck, 605 BEAM4 elements for the towers, 392 LINK11 elements for the cables, 64 LINK8 elements for the stabilizing cables, and 8 LINK8 elements for restraints of the bridge deck. A total of 5,610 nodes are used in total. All degrees of freedom are assumed to be fixed at the base of each tower. The rocker bearings at both the Ting Kau Pier and Tsing Yi Abutment allow translational and rotational movements in the longitudinal vertical planes but no movements in the transverse direction. In order to establish the baseline FE model for long term monitoring and condition evaluation, model updating is implemented by minimizing the discrepancy between the measured responses and the responses obtained from the FE model.

4.1 Ambient modal analysis

The modal properties of Ting Kau Bridge can be extracted from the acceleration data collected by the Wind and Structural Health Monitoring System on the bridge (Fig. 5) (Wong 2004, Au *et al.* 2003, Mao *et al.* 2018). The methods

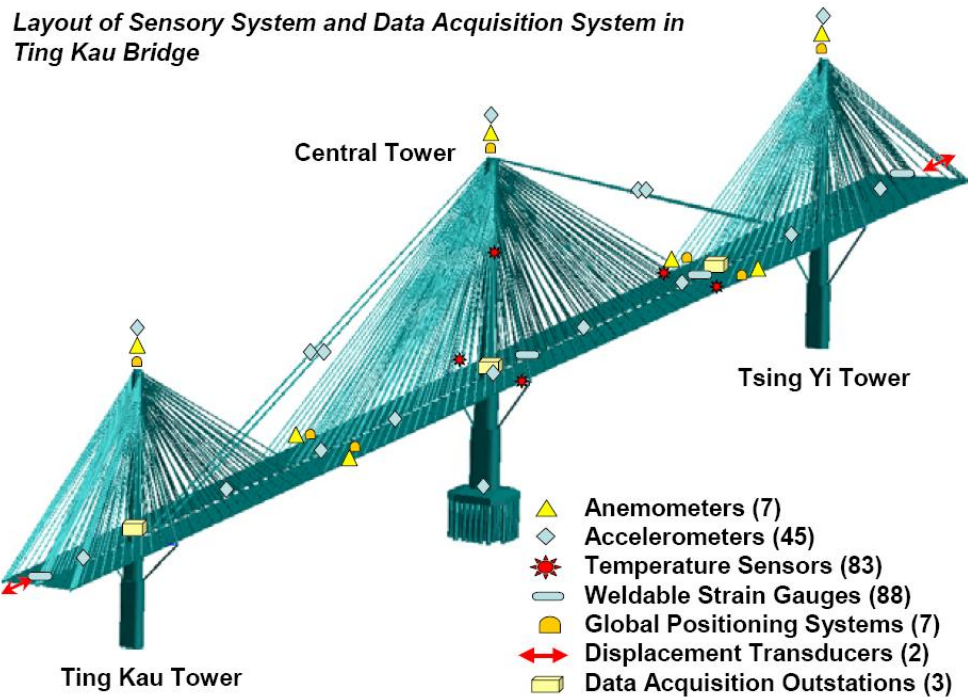


Fig. 5 Example 2: Wind and structural health monitoring system on Ting Kau Bridge

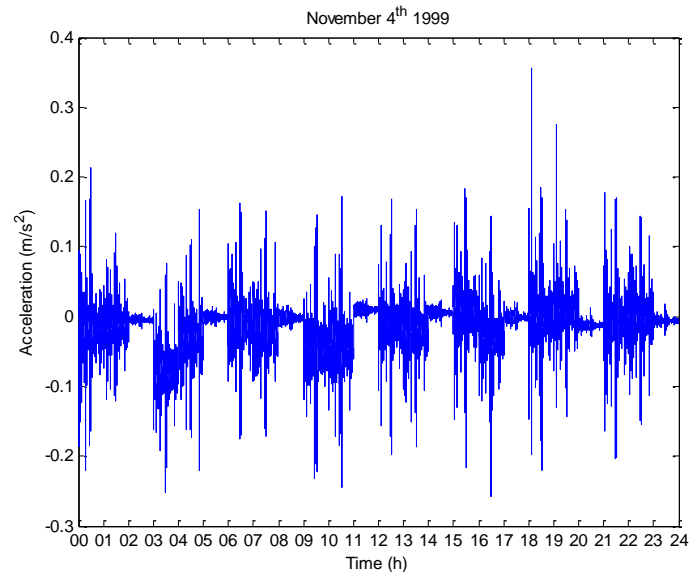


Fig. 6 Example 2: Acceleration data on Nov 4, 1999 at selected location

of ambient modal analysis used here include the power spectrum density transmissibility approach in the frequency domain (Yan and Ren 2012) and stochastic system identification in the time domain (Peeters and De Roeck 2001, Bakir 2011). Using the acceleration data measured on November 4, 1999 at selected locations as shown in Fig. 6, the power spectrum density transmissibility approach is applied to a record lasting several minutes. The modal frequencies are identified from the peaks of averaged normalized inverse transmissibility shown in Fig. 7 and listed in Table 12. The package MACEC v3.1 (Reynders *et*

al. 2011) for data pre-processing, modal parameter identification and post-processing is then used to prepare the stabilization diagram shown in Fig. 8. Various symbols in the figure denote computational results in respect of the systematic model order versus frequency, i.e. “⊕” for a stable mode, “·v” for a stable frequency and mode shape, “·d” for a stable frequency and damping, and “·f” for a stable frequency. Among the first six mode shapes identified as shown in Table 13, the first and fifth modes are vertical, while the others are lateral. These frequencies will be adopted as the objective values for further updating.

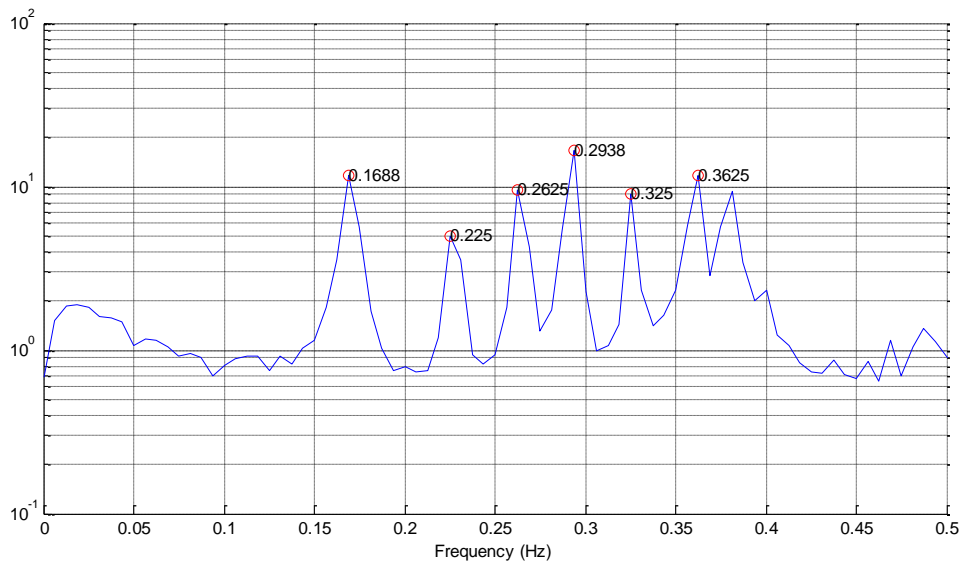


Fig. 7 Example 2: Modal frequencies extracted by power spectrum density transmissibility

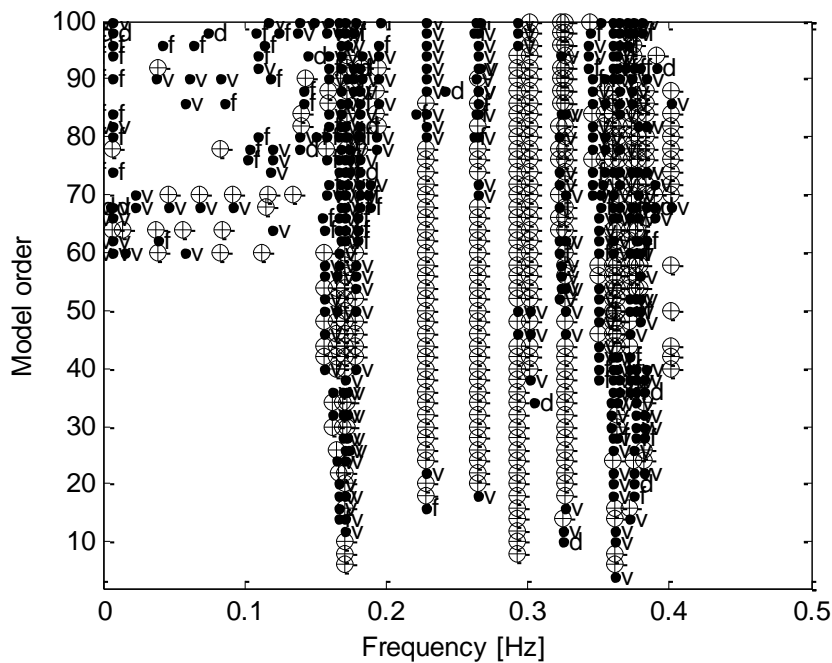


Fig. 8 Example 2: Stabilization diagram based on acceleration data of Nov 4, 1999

Note: \oplus denotes a stable mode, $\cdot v$ a stable frequency and mode shape, $\cdot d$ a stable frequency and damping, and $\cdot f$ a stable frequency

Table 12 Example 2: Modal frequencies extracted by power spectrum density transmissibility

Order	Frequency(Hz)	Mode
1	0.1688	Vertical
2	0.2250	Lateral
3	0.2625	Lateral
4	0.2938	Lateral
5	0.3250	Lateral
6	0.3625	Vertical

4.2 Static loading tests

To provide additional references in the form of influence lines and surfaces for stress and displacement for structural health monitoring of Ting Kau Bridge, a series of vehicular loading tests were carried out by the Highways Department of Hong Kong Government with temporary traffic closure. These tests were scheduled during the periods of March 8-19, 1999 and March 27-30, 2007. The movements of locations ‘D1’ and ‘D2’ at deck level of the bridge as shown in Fig. 3 are monitored by the GPS system.

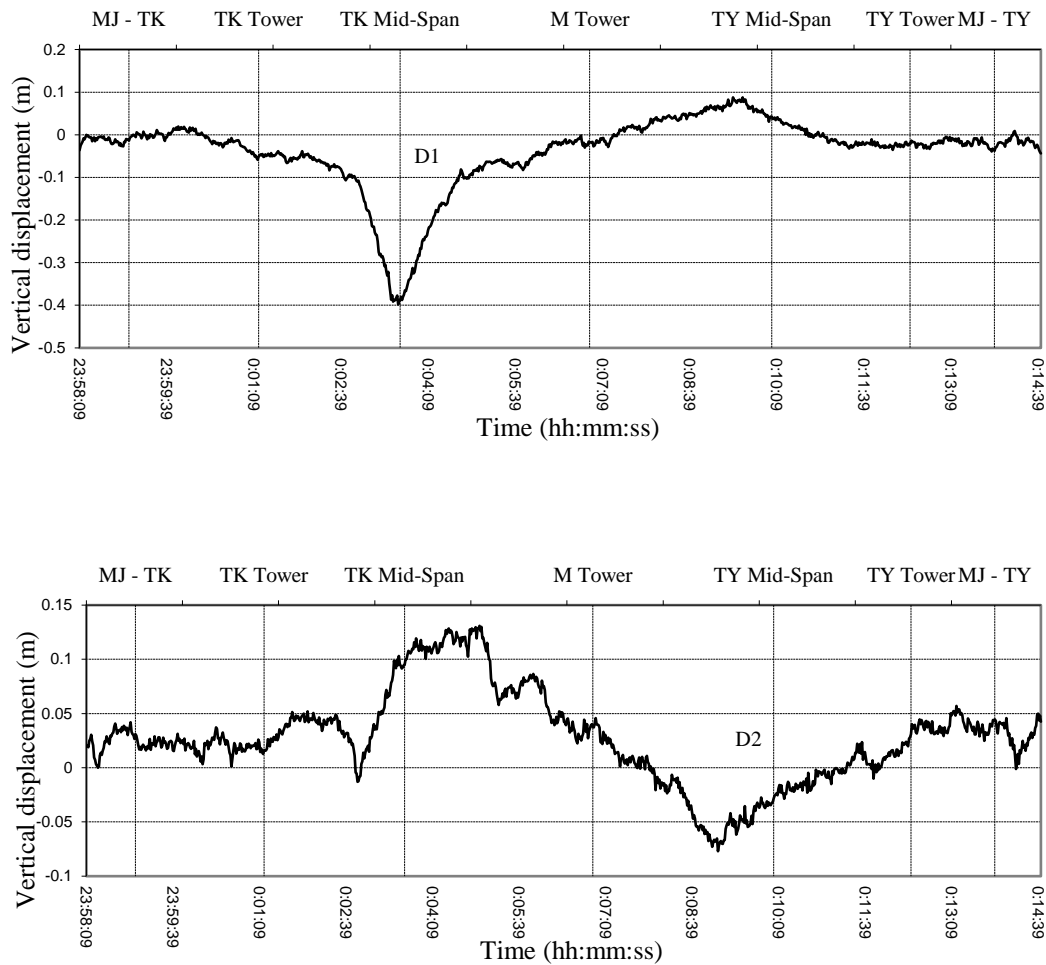


Fig. 9 Example 2: Measured deck displacements at locations 'D1' and 'D2'

Table 13 Example 2: Modal frequencies extracted by stochastic system identification

Order	Frequency (Hz)	Mode	Damping ratio (%)
1	0.17036	Vertical	1.02300
2	0.22817	Lateral	0.30142
3	0.26467	Lateral	0.57163
4	0.29240	Lateral	0.53315
5	0.32548	Lateral	0.46523
6	0.37410	Vertical	0.64084

In one of the test cases, a heavy transporter with two tractors and a 7-axle trailer travelled south at a crawling speed of 5 km/hr across the bridge with the centre of gravity on the north-bound hard shoulder. The axle weight distribution of the transporter is listed in Table 14. The measured deck displacements at 'D1' and 'D2' are shown in Fig. 9.

The movement of the heavy transporter is again simulated by ANSYS Multiphysics. In particular, when each axle load moves along a traffic lane, the transverse

equivalent load system that comprises the nodal forces and moments is applied to the two longitudinal girders supporting the carriageway. Similarly, each moving load along a longitudinal girder can be modelled by using the equivalent time-varying nodal forces and moments on the element carrying the moving load. In view of the vehicle speed of 5 km/hr, the test was not really static, and hence transient analysis is carried out to obtain the displacements at 'D1' and 'D2' as shown in Fig. 10. Rayleigh damping is assumed with the corresponding coefficients calculated using the damping ratios of the first and second vertical modes, which are 1.023% and 0.64084% respectively as shown in Table 13. Then the mass- and stiffness-proportional damping coefficient are obtained as 0.01975 and 0.001878 respectively.

4.3 Parameter selection and model updating

In order to select the effective model parameters of the bridge in Table 15 for updating, the F-test is conducted to evaluate their respective significance. The orthogonal method of experimental design as shown in Table 16 is used

Table 14 Example 2: Axle weight distribution of transporter (tonnes)

Vehicle Type	Tractor			Trailer							Tractor		
Car Reg. No.	LN2387			46983T							LN2387		
	axle1	axle2	axle3	axle1	axle2	axle3	axle4	axle5	axle6	axle7	axle1	axle2	axle3
Right (driver)	5.000	8.405	8.405	7.523	7.523	7.523	7.523	7.523	7.523	7.523	5.000	8.295	8.295
Left (passenger)	5.000	8.405	8.405	7.523	7.523	7.523	7.523	7.523	7.523	7.523	5.000	8.295	8.295
Total per axle	10.00	16.81	16.81	15.05	15.05	15.05	15.05	15.05	15.05	15.05	10.00	16.59	16.59
Total Vehicle	43.62			105.32							43.18		

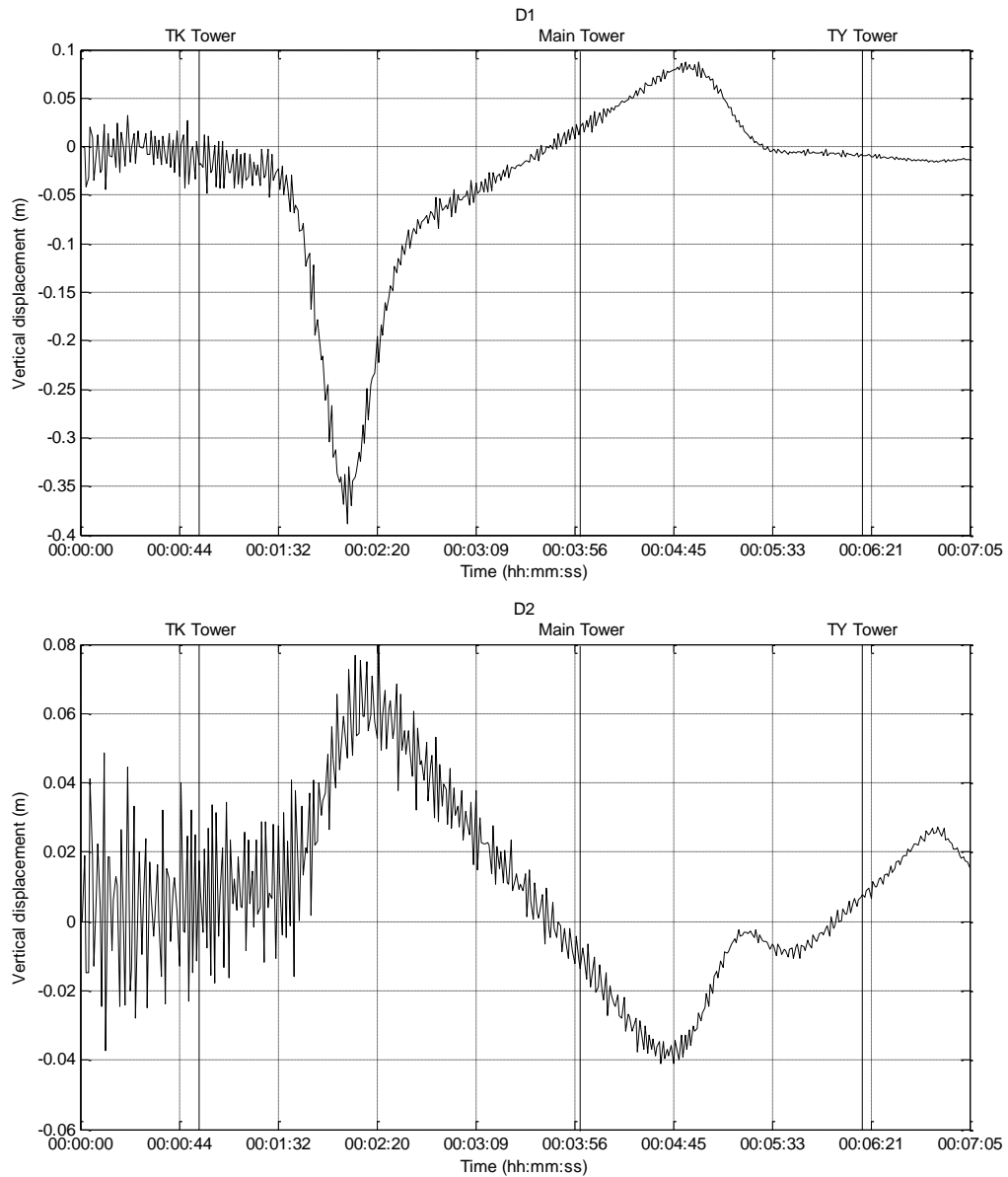


Fig. 10 Example 2: Simulated deck displacements at locations ‘D1’ and ‘D2’

for the analysis of variance because the full factorial design of experiment is not advisable. Any 14 columns of the table can be chosen to sample the points globally. Fig. 11 shows that parameters X1, X2, X8, X12, X13 and X14 mainly affect the first 6 frequencies and the deck displacements ‘D1’ and ‘D2’ at monitoring points. The allowable bounds

of the 6 parameters selected are listed in Table 17. For the Young’s moduli of the tower, the cross girder and the main girder, 30% variation is allowed, while 20% variation is permitted for the density of the three towers as well as the area of the main girder. As the cross section of the main girder may be non-uniform, any representative cross section

can be chosen to form the surrogate model with possible variations. For the second moments of area of the main girders, the bounds are set to be 30% due to the complexity of the component and the simplification in the development of FE model.

Table 15 Example 2: Selected parameters for model updating

Parameters	Notation	Bounds (%)
Young's modulus of tower	X1	±10
Density of tower	X2	±10
Young's modulus of connecting girder	X3	±10
Density of connecting girder	X4	±10
Cross sectional area of connecting girder	X5	±10
Second moment of area I_y of connecting girder	X6	±10
Second moment of area I_z of connecting girder	X7	±10
Young's modulus of cross girder and main girder	X8	±10
Cross sectional area of cross girder	X9	±10
Second moment of area I_y of cross girder	X10	±10
Second moment of area I_z of cross girder	X11	±10
Cross sectional area of main girder	X12	±10
Second moment of area I_y of main girder	X13	±10
Second moment of area I_z of main girder	X14	±10

Table 16 Example 2: Orthogonal experimental design of 15 factors

Level	Factor														
	1	2	3	4	5	6	7	8	9	10	11	12	13	14	15
1	1	1	1	1	1	1	1	1	1	1	1	1	1	1	1
2	1	1	1	1	1	1	1	2	2	2	2	2	2	2	2
3	1	1	1	2	2	2	2	1	1	1	1	2	2	2	2
4	1	1	1	2	2	2	2	2	2	2	2	1	1	1	1
5	1	2	2	1	1	2	2	1	1	2	2	1	1	2	2
6	1	2	2	1	1	2	2	2	2	1	1	2	2	1	1
7	1	2	2	2	2	1	1	1	1	2	2	2	2	1	1
8	1	2	2	2	2	1	1	2	2	1	1	1	1	2	2
9	2	1	2	1	2	1	2	1	2	1	2	1	2	1	2
10	2	1	2	1	2	1	2	2	1	2	1	2	1	2	1
11	2	1	2	2	1	2	1	1	2	1	2	2	1	2	1
12	2	1	2	2	1	2	1	2	1	2	1	1	2	1	2
13	2	2	1	1	2	2	1	1	2	2	1	1	2	2	1
14	2	2	1	1	2	2	1	2	1	1	2	2	1	1	2
15	2	2	1	2	1	1	2	1	2	2	1	2	1	1	2
16	2	2	1	2	1	1	2	2	1	1	2	1	2	2	1

Table 17 Example 2: Selected updating parameters and allowable bounds

No.	Model parameters	Allowable bounds (%)
1	Young's modulus of tower	±30
2	Density of tower	±20
3	Young's modulus of cross girder and main girder	±30
4	Cross sectional area of main girder	±20
5	Second moment of area I_y of main girder	±30
6	Second moment of area I_z of main girder	±30

Table 18 Example 2: Results of initial and updated FE models

Modal frequencies					
Order	Initial FE model (Hz)	MACEC (99Mar1104) (Hz)	Error (%)	Updated FE model (Hz)	Error (%)
1	0.16358	0.17036	-3.98	0.16520	-3.03
2	0.23957	0.22817	5.00	0.22643	-0.76
3	0.25472	0.26467	-3.76	0.26709	0.91
4	0.28627	0.29240	-2.10	0.29534	1.01
5	0.29542	-	-	0.30268	-
6	0.30194	0.32548	-7.23	0.30956	-4.89
7	0.31984	-	-	0.31565	-
8	0.34401	0.37410	-8.04	0.33728	-9.84

Vertical displacements					
Location	Initial FE model (m)	Load test (m)	Error (%)	Updated FE model (m)	Error (%)
D1	-0.37766	-0.3980	-5.11	-0.41659	4.67
D2	-0.03887	-0.0771	-49.59	-0.057807	-25.02

In the optimization process, the objective function is expressed in terms of the residuals between the measured responses (including the first six frequencies and maximum displacements of 'D1' and 'D2' during the load test) and the corresponding theoretical responses with all the objective values non-dimensionalized. The corresponding weighting coefficients are taken as [10 8 4 2 1 4 2] based on the sensitivity study and also engineering judgment. The choice of weighting coefficients should reflect the nature of this complex structure and address various characteristics. The weights for the third and higher frequencies are chosen to be less than those for the first two. The weight for the maximum displacement should not be too large, or else the accuracy of frequencies will suffer. As shown in Table 18, the updated model performs better than the initial model. The adjustments of parameters as shown in Table 19 are all within the permitted range. The updated model can thus be taken as a baseline model for further fatigue analysis.

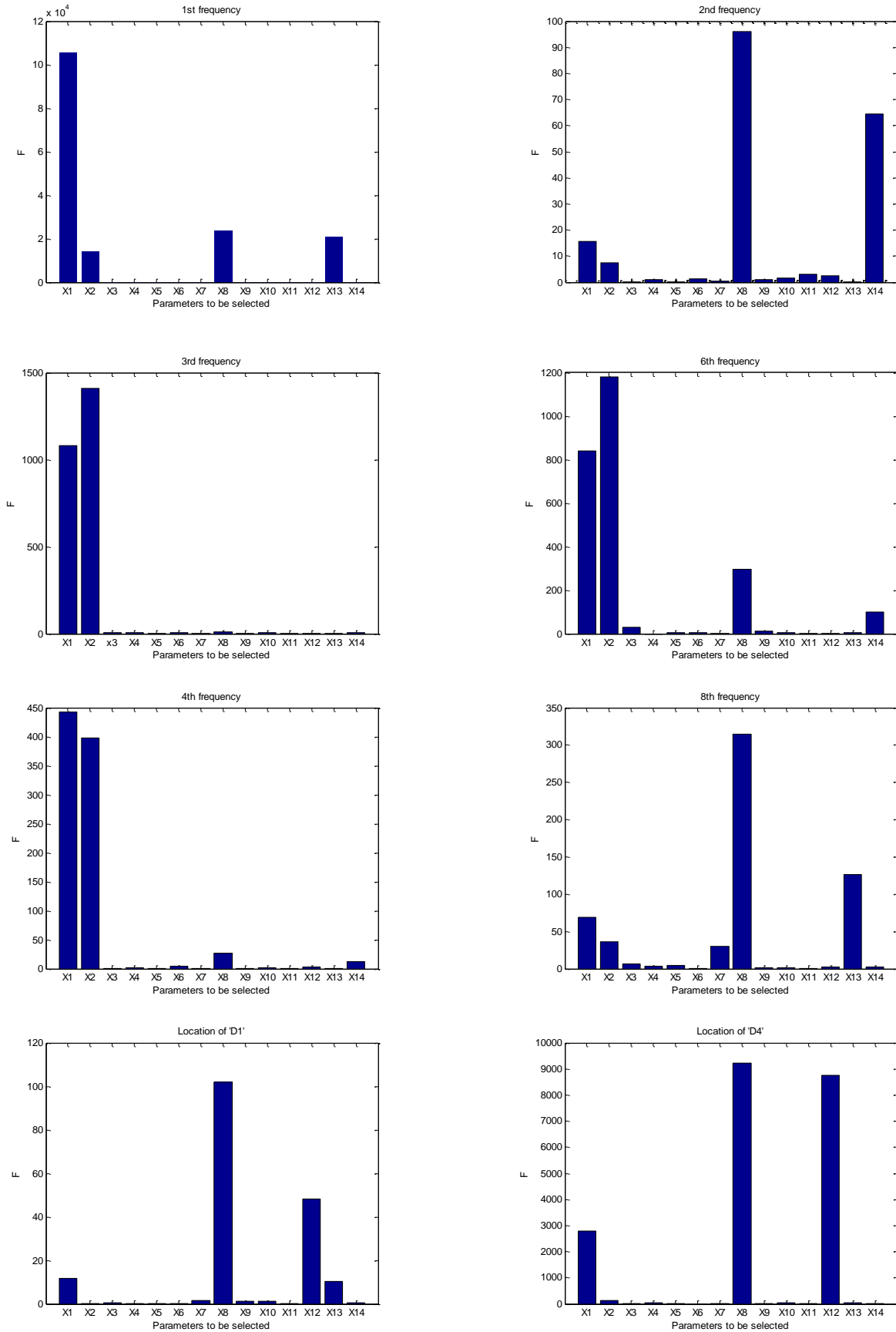


Fig. 11 Example 2: Eigenvalue sensitivity and sensitivity of deck displacements to model parameters considered

Table 19 Example 2: Updated model parameters

Parameters	Initial estimation	Updated value	Adjustment (%)
Young's modulus of tower (GPa)	30.2	38.6	27.95
Density of tower (kg/m ³)	2500	2703	8.12
Young's modulus of cross girder and main girder (GPa)	200	149.15	-25.43
Cross sectional area of main girder (m ²)	0.6642	0.7159	7.78
Second moment of area I_y of main girder (m ⁴)	0.1419	0.1304	-8.14
Second moment of area I_z of main girder (m ⁴)	115.0387	129.6481	12.70

5. Fatigue life considering mean stress effect

Fatigue has been one of the most critical forms of damage for cable-supported bridges with steel components. In the assessment of remaining fatigue lives, a crucial step is to determine the fatigue stress spectra. Usually, the fatigue stress spectra of bridges can be obtained through field measurements from structural health monitoring systems, which are able to record the responses for fatigue assessment and long-term performance prediction. However, these systems are always expensive, and there are a lot of structural components that are difficult to install strain gauges. Therefore it is desirable to develop an effective method to obtain fatigue stress spectra of inaccessible structural details. The standard fatigue vehicle (SFV) is then used to estimate the damage accumulation at fatigue-critical locations of the bridge for estimation of the fatigue life.

The equivalent number of SFVs converted from different types of road vehicles running on the j -th traffic lane can be calculated (Au *et al.* 2011). The equivalent annual SFV spectrum of Ting Kau Bridge in 2007 is shown in Table 20 where k_w is the ratio of gross vehicle weight of road vehicle to the weight of the SFV. Based on Miner's rule for fatigue prediction, the fatigue life L_F based on the initial finite element model or the baseline model is calculated considering the mean stress effect (Zhang and Au 2013). Linear strain gauges 'SSGLE04' and 'SSGLW04' have been installed on the first and fourth bridge girders respectively in the vicinity of cable anchorages at location 'L' as shown in Fig. 3. Their fatigue lives can be obtained as shown in Tables 21 and 22, where R is the stress ratio of the minimum stress and maximum stress and N is the number of cycles to failure. The measured strain time histories on Nov 22, 2007 are shown in Fig. 12. Using the rain-flow counting method, the fatigue lives obtained from the data of 'SSGLE04' and 'SSGLW04' are 283 years and 208 years, respectively, which agree well with the numerical predictions using the baseline model.

Table 20 Equivalent annual SFV spectrum of Ting Kau Bridge in 2007 (Au *et al.* 2011)

k_w	Ting Kau Bound (million)			Tsing Yi Bound (million)		
	Slow lane	Middle lane	Fast lane	Slow lane	Middle lane	Fast lane
0.0938	14	34	22	17	29	24
0.1875	122	147	30	52	137	29
0.3125	1236	711	40	415	387	12
0.4375	7568	5698	152	4909	3625	38
0.5625	34429	19321	120	28100	12602	30
0.6875	54649	25788	128	83285	15629	47
0.8125	59038	23386	150	111197	21383	53
0.9375	79665	31396	295	121102	20325	59
1.0625	120255	30604	469	139155	25963	65
1.1875	151228	30863	524	181704	32812	66
1.3125	153603	32172	526	209838	34462	74
1.4375	145665	20864	203	254163	44404	55
1.5625	143889	11241	363	271769	39721	37
1.6875	150321	5091	369	321701	22059	14
1.8125	155334	2210	137	242947	10856	20
1.9375	119778	464	328	174302	8000	0
2.0625	81064	149	37	120327	6233	0
2.1875	52894	50	50	104886	4859	0
2.3125	36108	0	0	88947	4034	0
2.4375	49131	0	86	137585	33643	0
Total	1595989	240189	4030	2596401	341161	623

6. Conclusions

In order to minimize the discrepancies between results from the FE model and field measurements from the real bridge, a model updating method based on Kriging surrogate model is proposed for cable-stayed bridges in this paper. The application of Kriging surrogate model is more flexible than the conventional response surface surrogate model. The efficiency and accuracy of the proposed method is firstly verified by a simple hypothetical cable-stayed bridge. With verification of the correctness, practicability and high efficiency of the method, it is adopted to calibrate the FE model of Ting Kau Bridge using information from the static and dynamic field tests. As there is no need for each iteration to invoke the FE package for re-analysis with various parameters updated, the proposed method is much more computationally efficient. Results show that this method based on Kriging surrogate model is promising since it can provide satisfactory solutions without excessive computations. The updated model can be taken as a reference baseline model for further structural analysis. Then fatigue analysis can be carried out employing the updated model with the equivalent number of standard fatigue vehicles considering the mean stress effect. The fatigue lives estimated numerically in this manner compare favourably with those based on the strain data from measurements of the Wind and Structural Health Monitoring System in operation. The mean stress effect should be properly taken into account to provide reliable fatigue life prediction with baseline FE model.

Table 21 Example 2: Fatigue life calculation for ‘SSGLW04’ using SFV method

(a) Before updating (Dead load stress: -1.9838 MPa)

Parameters	Lane 1	Lane2	Lane 3	Lane 4	Lane 5	Lane 6
Stress range (MPa)	16.6977	11.8145	7.2892	2.5952	1.8591	1.4077
<i>R</i>	-0.2845	-0.3650	-0.5779	-37.5582	0.2600	0.4359
Net tensile stress	Positive	Positive	Positive	Positive	Negative	Negative
Revised stress range (MPa)	18.4078	12.8513	7.6798	1.3527	-	-
<i>N</i>	4.8450×10^8	2.9212×10^9	3.8331×10^{10}	2.2610×10^{14}	-	-
Fatigue life (year)	197					

(b) After updating (Dead load stress: -1.7421 MPa)

Parameters	Lane 1	Lane 2	Lane 3	Lane 4	Lane 5	Lane 6
Stress range (MPa)	15.0927	10.5975	6.4949	2.1513	1.5142	1.1688
<i>R</i>	-0.1669	-0.1811	-0.2264	-0.8166	-1.6808	-3.9084
Net tensile stress	Positive	Positive	Positive	Positive	Positive	Positive
Revised stress range (MPa)	16.9939	11.9007	7.2334	2.1973	1.4196	0.9591
<i>N</i>	7.2249×10^8	4.2898×10^9	5.1712×10^{10}	1.9992×10^{13}	1.7761×10^{14}	1.2618×10^{15}
Fatigue life (year)	294					

Table 22 Example 2: Fatigue life calculation for ‘SSGLE04’ using SFV method

(a) Before updating: (Dead load stress: -3.307 MPa)

Parameters	Lane 1	Lane2	Lane 3	Lane 4	Lane 5	Lane 6
Stress range (MPa)	1.3575	1.8105	2.5426	7.2376	11.7564	16.6311
<i>R</i>	0.6406	0.5229	0.3328	-1.2160	-0.6122	-0.4304
Net tensile stress	Negative	Negative	Negative	Positive	Positive	Positive
Revised stress range (MPa)	-	-	-	7.0760	12.3279	17.9050
<i>N</i>	-	-	-	5.7725×10^{10}	3.5963×10^9	5.5645×10^8
Fatigue life (year)	140					

(b) After updating: (Dead load stress: -2.997 MPa)

Parameters	Lane 1	Lane2	Lane 3	Lane 4	Lane 5	Lane 6
Stress range (MPa)	1.1268	1.4738	2.1081	6.4517	10.5534	15.0432
<i>R</i>	0.4783	0.3235	0.0405	-0.6098	-0.3748	-0.2934
Net tensile stress	Negative	Negative	Negative	Positive	Positive	Positive
Revised stress range (MPa)	-	-	-	6.7675	11.4614	16.5586
<i>N</i>	-	-	-	7.2137×10^{10}	5.1774×10^9	8.2259×10^8
Fatigue life (year)	207					

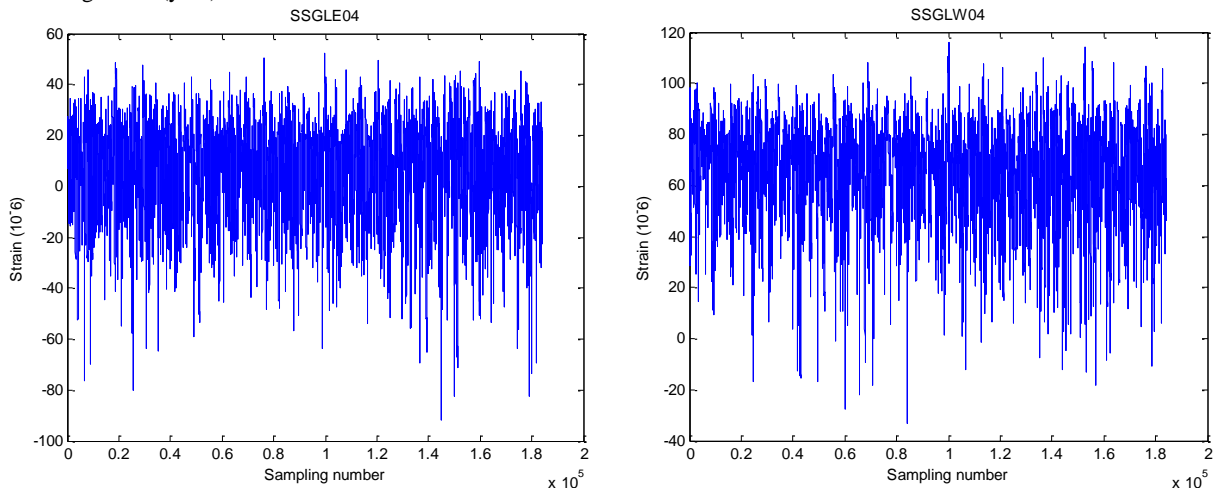


Fig. 12 Example 2: Data segment of strain time histories of ‘SSGLE04’ and ‘SSGLW04’ on Nov 22, 2007

Acknowledgments

The authors gratefully acknowledge the Highways Department of the Hong Kong Government for assistance received in producing this paper as well as permission of its publication. Any opinions expressed or conclusions reached in the paper are entirely of the authors. Financial support from the National Natural Science Foundation of China under Grant No. 51608162 is acknowledged.

References

- Ahmadian, H., Gladwell, G.M.L. and Ismail, F. (1997), "Parameter selection strategies in finite element model updating", *J. Vib. Acoust.*, **119**(1), 37-45. <https://doi.org/10.1115/1.2889685>.
- ANSYS Multiphysics 12.0. (2009), *Structural Analysis Guide*, Canonsburg.
- Arora, V. (2014), "FE model updating method incorporating damping matrices for structural dynamic modifications", *Struct. Eng. Mech.*, **52**(2), 261-274. <https://doi.org/10.12989/sem.2014.52.2.261>.
- Au, F.T.K., Tham, L.G., Lee, P.K.K., Su, C., Han, D.J., Yan, Q.S. and Wong, K.Y. (2003), "Ambient vibration measurements and finite element modelling for the Hong Kong Ting Kau Bridge", *Struct. Eng. Mech.*, **15**(1), 115-134. <https://doi.org/10.12989/sem.2003.15.1.115>.
- Au, F.T.K., Lou, P., Li, J., Jiang, R.J., Zhang, J., Leung, C.C.Y., Lee, P.K.K., Lee, J.H., Wong, K.Y. and Chan, H.Y. (2011), "Simulation of vibrations of Ting Kau Bridge due to vehicular loading from measurements", *Struct. Eng. Mech.*, **40**(4), 471-488. <https://doi.org/10.12989/sem.2011.40.4.471>.
- Bakir, P.G. (2011), "The combined deterministic stochastic subspace based system identification in buildings", *Struct. Eng. Mech.*, **38**(3), 105-112. <https://doi.org/10.12989/sem.2011.38.3.315>.
- Basaga, H.B., Bayraktar, A. and Kaymaz, I. (2012), "An improved response surface method for reliability analysis of structures", *Struct. Eng. Mech.*, **42**(2), 175-189. <https://doi.org/10.12989/sem.2012.42.2.175>.
- Cheng, J. (2010), "Determination of cable forces in cable-stayed bridges constructed under parametric uncertainty", *Eng. Computation*, **27**(3), 301-321. <https://doi.org/10.1108/02644401011029907>.
- Dubourg, V., Sudret, B. and Bourinet, J.-M. (2011), "Reliability based design optimization using kriging surrogates and subset simulation", *Struct. Multidiscip. O.*, **44**, 673-690. <https://doi.org/10.1007/s00158-011-0653-8>.
- Fang, K.T. and Wang, Y. (1993), *Number-theoretic methods in statistics* (CRC Press).
- Friswell, M.I. and Mottershead, J.E. (1995), *Finite element model updating in structural dynamics* (Springer Science & Business Media).
- Gao, H.Y., Guo, X.L. and Hu, X.F. (2012), "Crack identification based on Kriging surrogate model", *Struct. Eng. Mech.*, **41**(1), 25-41. <https://doi.org/10.12989/sem.2012.41.1.025>.
- Gaspar, B., Palos Teixeira, A. and Guedes Soares, C. (2014), "Assessment of the efficiency of Kriging surrogate models for structural reliability analysis", *Probabilist. Eng. Mech.*, **37**, 24-34. <https://doi.org/10.1016/j.probenmech.2014.03.011>.
- Hwang, Y., Jin, S.S., Jung, H.Y., Kim, S., Lee, J.J. and Jung, H.J. (2018), "Experimental validation of FE model updating based on multi-objective optimization using the surrogate model", *Struct. Eng. Mech.*, **65**(2), 173-181. <https://doi.org/10.12989/sem.2018.65.2.173>.
- Jaishi, B., Kim, H.J., Kim, M.K., Ren, W.X. and Lee, S.H. (2007), "Finite element model updating of concrete filled steel tubular arch bridge under operational condition using modal flexibility", *Mech Syst Signal Pr*, **21**(6), 2406-2426. <https://doi.org/10.1016/j.ymssp.2007.01.003>.
- Jaishi, B. and Ren, W.X. (2007), "Finite element model updating based on eigenvalue and strain energy residuals using multiobjective optimisation technique", *Mech Syst Signal Pr*, **21**(5), 2295-2317. <https://doi.org/10.1016/j.ymssp.2006.09.008>.
- Kalita, K., Nasre, P., Dey, P. and Haldar, S. (2018), "Metamodel based multi-objective design optimization of laminated composite plates", *Struct. Eng. Mech.*, **67**(3), 301-310. <https://doi.org/10.12989/sem.2018.67.3.301>.
- Khodaparast, H.H., Mottershead, J.E. and Badcock, K.J. (2011), "Interval model updating with irreducible uncertainty using the Kriging predictor", *Mech Syst Signal Pr*, **25**(4), 1204-1226. <https://doi.org/10.1016/j.ymssp.2010.10.009>.
- Lertsima, C., Chaisomphob, T. and Yamaguchi, E. (2004), "Three-dimensional finite element modeling of a long-span cable-stayed bridge for local stress analysis", *Struct. Eng. Mech.*, **18**(1), 113-124. <https://doi.org/10.12989/sem.2004.18.1.113>.
- Li, J., Hao, H. and Chen, Z.W. (2017), "Damage identification and optimal sensor placement for structures under unknown traffic-induced vibrations", *J. Aerospace Eng.*, **30**(2), B4015001. [http://dx.doi.org/10.1061/\(ASCE\)AS.1943-5525.0000550](http://dx.doi.org/10.1061/(ASCE)AS.1943-5525.0000550).
- Li, R., Lin, D.K.J. and Chen, Y. (2004), "Uniform design: design, analysis and applications", *Int. J. Mater. Prod. Tec.*, **20**(1-3), 101-114. <https://doi.org/10.1504/IJMPT.2004.003915>.
- Lophaven, S.N., Nielsen, H.B. and Søndergaard, J. (2002), *DACE: a Matlab Kriging toolbox* (Citeseer).
- Mao, J.X., Wang, H., Feng, D.M., Tao, T.Y. and Zheng, W.Z. (2018), "Investigation of dynamic properties of long-span cable-stayed bridges based on one-year monitoring data under normal operating condition", *Struct. Control Health Monit.*, **25**(5), e2146. <https://doi.org/10.1002/stc.2146>.
- Matta, E. and De Stefano, A. (2012), "Robust finite element model updating of a large-scale benchmark building structure", *Struct. Eng. Mech.*, **43**(3), 371-394. <https://doi.org/10.12989/sem.2012.43.3.371>.
- MATLAB 8.0. In. (2012), Natick, Massachusetts, United States: The MathWorks, Inc.
- Montgomery, D.C. (2017), *Design and analysis of experiments* (John Wiley & sons).
- Mottershead, J.E. and Friswell, M.I. (1993), "Model updating in structural dynamics: a survey", *J. Sound Vib.*, **167**(2), 347-375. <https://doi.org/10.1006/jsvi.1993.1340>.
- Myers, R.H. (1999), "Response surface methodology—current status and future directions", *J. Qual. Technol.*, **31**(1), 30-44. <https://doi.org/10.1080/00224065.1999.11979891>.
- Peeters, B. and De Roeck, G. (2001), "Stochastic system identification for operational modal analysis: a review", *J. Dyn. Syst.-T. Asme*, **123**(4), 659-667. <https://doi.org/10.1115/1.1410370>.
- Qin, S.Q., Hu, J., Zhou, Y.L., Zhang, Y.Z. and Kang, J.T. (2019), "Feasibility study of improved particle swarm optimization in kriging metamodel based structural model updating", *Struct. Eng. Mech.*, **70**(5), 513-524. <https://doi.org/10.12989/sem.2019.70.5.513>.
- Ren, W.X. and Chen, H.B. (2010), "Finite element model updating in structural dynamics by using the response surface method", *Eng. Struct.*, **32**(8), 2455-2465. <https://doi.org/10.1016/j.engstruct.2010.04.019>.
- Ren, W.X., Fang, S.E. and Deng, M.Y. (2010), "Response surface-based finite-element-model updating using structural static responses", *J. Eng. Mech.*, **137**(4), 248-257. [https://doi.org/10.1061/\(asce\)em.1943-7889.0000223](https://doi.org/10.1061/(asce)em.1943-7889.0000223).
- Reynders, E., Schevenels, M. and De Roeck, G. (2011), "MACEC

- 3.2: A Matlab toolbox for experimental and operational modal analysis-User's manual", *Katholieke Universiteit, Leuven*.
- Sacks, J., Welch, W.J., Mitchell, T.J. and Wynn, H.P. (1989), "Design and analysis of computer experiments", *Stat. Sci.*, **4**(4), 409-423. <https://doi.org/10.1214/ss/1177012413>.
- Sahin, A. and Bayraktar, A. (2014), "Computational finite element model updating tool for modal testing of structures", *Struct. Eng. Mech.*, **51**(2), 229-248. <https://doi.org/10.12989/sem.2014.51.2.229>.
- Sakata, S.-I., Ashida, F. and Zako, M. (2008), "Approximate structural optimization using kriging method and digital modeling technique considering noise in sampling data", *Comput. Struct.*, **86**(13-14), 1477-1485. <https://doi.org/10.1016/j.compstruc.2007.05.007>.
- Shao, T.F. and Krishnamurty, S. (2008), "A clustering-based surrogate model updating approach to simulation-based engineering design", *J. Mech. Design*, **130**(4), 041101. <https://doi.org/10.1115/1.2838329>.
- Simpson, T.W., Mistree, F., Korte, J.J. and Mauery, T.M. (1998), "Comparison of response surface and Kriging models for multidisciplinary design optimization", In *7th AIAA/USAF/NASA/ISSMO Symposium on Multidisciplinary Analysis and Optimization*, 4755.
- Simpson, T.W., Mauery, T.M., Korte, J.J. and Mistree, F. (2001), "Kriging models for global approximation in simulation-based multidisciplinary design optimization", *AIAA journal*, **39**(12), 2233-2241. <https://doi.org/10.2514/3.15017>.
- Vahidi, M., Vahdani, S., Rahimian, M., Jamshidi, N. and Kanee, A.T. (2019), "Evolutionary-base finite element model updating and damage detection using modal testing results", *Struct. Eng. Mech.*, **70** (3), 339-350. <https://doi.org/10.12989/sem.2019.70.3.339>.
- Wei, F.S. (1990), "Analytical dynamic model improvement using vibration test data", *AIAA journal*, **28**(1), 175-177. <https://doi.org/10.2514/3.10371>.
- Wong, K.Y. (2004), "Instrumentation and health monitoring of cable-supported bridges", *Struct. Control Hlth.*, **11**(2), 91-124. <https://doi.org/10.1002/stc.33>.
- Xie, X., Yamaguchi, H. and Nagai, M. (1997), "Static behaviors of self-anchored and partially earth-anchored long-span cable-stayed bridges", *Struct. Eng. Mech.*, **5**(5), 767-774. <https://doi.org/10.12989/sem.1997.5.6.767>.
- Yan, W.J. and Ren, W.X. (2012), "Operational modal parameter identification from power spectrum density transmissibility", *Comput.-Aided Civ. Inf.*, **27**(3), 202-217. <https://doi.org/10.1111/j.1467-8667.2011.00735.x>.
- Zhang, J. and Au, F.T.K. (2013), "Effect of baseline calibration on assessment of long-term performance of cable-stayed bridges", *Eng. Fail. Anal.*, **35**, 234-246. <https://doi.org/10.1016/j.engfailanal.2013.01.031>.
- Zhang, J., Huang, H.W. and Phoon, K.K. (2012), "Application of the Kriging-based response surface method to the system reliability of soil slopes", *J. Geotech. Geoenviron.*, **139**(4), 651-655. [https://doi.org/10.1061/\(ASCE\)GT.1943-5606.0000801](https://doi.org/10.1061/(ASCE)GT.1943-5606.0000801).